J Appl Electrochem (2008) 38:767–775
DOI 10.1007/s10800-008-9506-6

ORIGINAL PAPER

Morphological and electrochemical investigation of RuO_2–Ta_2O_5 oxide films prepared by the Pechini–Adams method

Josimar Ribeiro · Michael S. Moats · Adalgisa R. De Andrade

Received: 30 March 2007 / Revised: 17 January 2008 / Accepted: 28 January 2008 / Published online: 14 February 2008

Abstract Preparation methods can profoundly affect the structural and electrochemical properties of electrocatalytic coatings. In this investigation, RuO_2–Ta_2O_5 thin films containing between 10 and 90 at.% Ru were prepared by the Pechini–Adams method. These coatings were electrochemically and physically characterized by cyclic voltammetry, scanning electron microscopy (SEM), energy dispersive X-ray spectroscopy (EDX), X-ray photoelectron spectroscopy (XPS) and X-ray diffraction (XRD). The composition and morphology of the oxide were investigated before and after accelerated life tests (ALT) by EDX and SEM. SEM results indicate typical mud-flat-cracking morphology for the majority of the films. High resolution SEMs reveal that pure oxide phases exhibit nanoporosity while binary compositions display a very compact structure. EDX analyses reveal considerable amounts of Ru in the coating even after total deactivation. XRD indicated a rutile-type structure for RuO_2 and orthorhombic structure for Ta_2O_5. XPS data demonstrate that the binding energy of Ta is affected by Ru addition in the thin films, but the binding energy of Ru is not likewise influenced by Ta. The stability of the electrodes was evaluated by ALT performed at 750 mA cm^{-2} in 80 °C 0.5 mol dm^{-3} H_2SO_4. The performance of electrodes prepared by the Pechini–Adams method is 100% better than that of electrodes prepared by standard thermal decomposition.

J. Ribeiro · A. R. De Andrade (✉)
Departamento de Química, Faculdade de Filosofia Ciências e Letras de Ribeirão Preto, Universidade de São Paulo, 14040-901 Ribeirao Preto, SP, Brazil
e-mail: ardandra@ffclrp.usp.br

M. S. Moats
Department of Metallurgical Engineering, University of Utah, Salt Lake City, UT, USA

Keywords Ruthenium and tantalum oxide · EDS · SEM · XPS · Pechini–Adams method

1 Introduction

The use of ceramic films consisting of RuO_2 and Ta_2O_5 has found many applications, such as solid state sensors, dynamic memory capacitors, hybrid capacitors, supercapacitors, and MOS (metal/oxide/semiconductor) transistors [1–6]. Moreover, the RuO_2–Ta_2O_5 system has recently been investigated by us [4], and we observed that it is much more stable than RuO_2–TiO_2 under galvanostatic conditions [7, 8].

Electrochemical properties (e.g., durability and electrocatalytic activity) of electrocatalytic coatings are associated with the microstructure of the active layer. The crystallite size depends on the solvent of the precursor [9] as well as on the nature of the precursor. DeBattisti et al. [10] have demonstrated that electrochemical properties are modified when the preparation method is changed. Therefore, alternative preparation methods could lead to the improvement of electrode performance.

Thin oxide films on Ti substrates, well-known DSA® (Dimensionally Stable Anodes), are frequently prepared by standard thermal decomposition (SD) of metallic precursor salts in aqueous or alcohol solution [4, 11, 12]. However, when thin films prepared by SD operate under severe conditions their total or partial deactivation can be observed in a short period of time [4, 13, 14]. Recently, Terezo and Pereira [15] demonstrated that Ti/RuO_2 electrodes prepared by the decomposition of polymeric precursors (DPP—Pechini–Adams method [16]) presented a higher electrocatalytic active area and increased durability than those prepared by SD.

The DPP-method consists of the thermal decomposition of metallic salts dissolved in a mixture of ethylene glycol

and citric acid [16–21]. This method is a good alternative to SD to overcome metal volatilization [19, 20] particularly in the preparation of ternary coating compositions containing SnO_2 [19, 20].

The aim of this work is to prepare electrodes coated with RuO_2 and Ta_2O_5 oxide films using DPP methodology and to examine the morphological, microstructural and electrochemical properties.

2 Experimental

2.1 Sample preparation

Thin film electrodes of nominal compositions: Ti/RuO_2–Ta_2O_5 (Ru:Ta—varying by 10 at.% Ru) were prepared by thermal decomposition of a polymeric precursor solution (DPP) [15–21]. The ruthenium polymeric precursor (Ru-resin) was prepared by first mixing citric acid (CA) (Merck) in ethylene glycol (EG) (Merck) at 60–65 °C. Then a ruthenium bearing solution ($RuCl_3 \times H_2O$ from Aldrich dissolved in isopropanol to obtain a concentration of 0.1 mol dm^{-3}) was added to achieve a molar ratio of CA:EG:Ru of 1:4:0.25. After the precursor salt was totally dissolved, the temperature of the mixture was raised to 90 °C and maintained at that level for 2–3 h while the mixture was stirred vigorously. The tantalum polymeric precursor (Ta-resin) was prepared in a similar way, but the molar ratio AC:EG:Ta was 1:5:0.2. The Ta was added as $Ta(OC_2H_5)_5$ obtained from ACROS. The final concentration of the each of the metal bearing polymeric precursors were determined by atomic absorption. The Ru-resin concentration was 3.5×10^{-3} mol of Ru/g of resin, while the Ta-resin concentration was 3.8×10^{-4} mol of Ta/g of resin.

Precursor mixtures were prepared for each electrode composition by mixing the appropriate amounts of Ru-resin and Ta-resin together. The precursor mixtures were applied by brushing to both sides of a pre-treated Ti-support [1, 5]. After application of the precursor mixture, the electrode was heated in air to 130–140 °C for 10 min to polymerize the coating, then fired at 450 °C for 5 min under a 5 dm^3 min^{-1} O_2-flux. The coat, polymerize and fire procedure was repeated until the desired nominal oxide loading (1.4–1.6 mg oxide cm^{-2}) was achieved. Upon achieving the target weight, the electrode received a 1 h bake at 450 °C under O_2-flux. Duplicate samples were prepared for each electrode composition. Details of the electrode preparation and final mounting are described elsewhere [22].

Powder samples with increasing at.% Ru nominal content (RuO_2–Ta_2O_5/Ru:Ta—varying by 10 at.% Ru) were also prepared by thermal decomposition of the polymeric precursor mixtures at 700 °C for 5 h in air.

2.2 Cell, equipment, and solutions

All solutions were prepared with 18.2 MΩ cm water, produced and purified by a Millipore-Milli-Q system. Electrochemical studies were performed using 0.5 mol dm^{-3} H_2SO_4 (Merck) as the supporting electrolyte.

The electrochemical experiments were conducted in a one-compartment cell with a main body of ~50 mL. The coated electrode serviced as the working electrode. Two 15 cm spiral platinized platinum wires were used as counter electrode. A reference hydrogen electrode (RHE) was utilized and positioned close to the working electrode by means of a Luggin-Haber capillary.

Electrochemical experiments were performed using a Solartron model 1480 multistat. Voltammetric curves were recorded in the 0.2–1.2 V vs. RHE potential range at a sweep rate of 100 mV s^{-1}.

Accelerated life tests (ALT) were performed under galvanostatic conditions at a high current density (750 mA cm^{-2}), and the temperature was maintained at 80 °C by means of a water thermostat. The period of time necessary for the electrode potential to achieve a value of 6 V vs. RHE was termed as the electrode lifetime. The electrode was considered inactive for OER at higher potentials. All electrochemical experiments were repeated at least twice.

2.3 Morphological characterization and surface composition

Surface morphology, microstructure, and elemental composition of the deposited oxide films were analyzed through scanning electron microscopy (SEM) and energy dispersive X-ray spectroscopy (EDS) using a Leica-Zeiss LEO 440 model SEM coupled to an Oxford 7060 model analyzer.

The XPS (X-ray photoelectron spectroscopy) surface analysis was performed on a Physical Electronics PHI-5600. Al mono 250 W at 1486.6 eV radiation was used to excite the photoelectrons from the sample. XPS spectra were obtained at a 45° angle of observation with respect to the surface of the photo-emitted electrons. The analytical spot size was ~800 micron.

X-ray diffraction analysis was performed by means of a Model D5005 Siemens instrument using CuK_α radiation ($\lambda = 1.5406$ Å). The following parameters were kept constant during X-ray analysis: 2θ range = 20°–85°, step = 0.03°, step time = 5 s, total analysis time = 1.8 h, and temperature = 27°C.

The phase composition of the RuO_2–Ta_2O_5 coating is rather complex and the analysis of its relevant position to the $K_{\alpha 1}$ monochromatic radiation was obtained by fitting the experimental angular range of interest to the

pseudo-Voigt 1 function per crystalline peak plus a background with the aid of a computer refinement program (Profile Plus Executable, Version 2.0, 1995 Siemens AG). The Ti peak positions were used as an internal standard to perform the calibration for peak shift. More procedural details are described elsewhere [4]. Crystallite sizes were obtained through the Debye–Scherrer equation: $D = K \times (\lambda \times 180^\circ/\pi)/\left[\sqrt{(\beta^2 - S^2) \times \cos\theta_\beta}\right]$ [23], where K is the shape factor (0.9 for spherical crystallite), λ is the wavelength of the radiation (1.5406 Å), S is the instrumental line broadening (0.001°), β is the reflection width at half-maximum intensity (FWHM), and θ_β is the angle at the maximum intensity.

Unit cell parameters were calculated by a computer program using the least squares method. Experimental 2θ and reflection parameters (hkl) were used as a first guess to obtain the fitting of the unit cell parameters.

3 Results and discussion

3.1 X-ray diffraction

Figure 1 shows the XRD patterns of the oxide mixture in powder form obtained by calcination of the precursor mixtures at 700 °C for 5 h. All samples show sharp and intense peaks attributed to RuO_2 and Ta_2O_5 phases. The XRD patterns indicate a rutile structure (110, 101, 200, and 211) with spatial group P42/mnm for RuO_2 and an orthorhombic structure for Ta_2O_5 [24]. This result was previously observed by us for the RuO_2–Ta_2O_5 system prepared by thermal decomposition of chloride precursor salts (e.g. SD method) [4].

It can be seen in Fig. 1 that a slight shift in peak positions occurs for binary oxides when compared with pure RuO_2 and Ta_2O_5 XRD patterns. This suggests a reciprocal solubility. Deconvolution of the peaks in the XRD of the RuO_2–Ta_2O_5 oxide mixture (Fig. 1) was performed as described elsewhere [4, 25]. Two saturated solid solutions of RuO_2 and Ta_2O_5 were formed between 10 and 90 at.% Ru loadings. The low (<10%) miscibility of RuO_2 and Ta_2O_5 is expected due to the distinctly different structures of the two oxides (tetragonal for RuO_2 and orthorhombic for Ta_2O_5) and different valences (+4 and +5, respectively). Additional, Ru and Ta do not satisfy the conditions outlined by Hume-Rothery et al. [26] for the formation of a substitutional solid solution. An interstitial solid solution could form at a lower concentration (e.g. below 10 at.%) but samples to confirm this were not produced in this study.

The XRD pattern obtained for RuO_2–Ta_2O_5 system in thin film form on a metallic Ti-base is shown in Fig. 2. For samples containing 40 at.% Ru or less, it was not possible

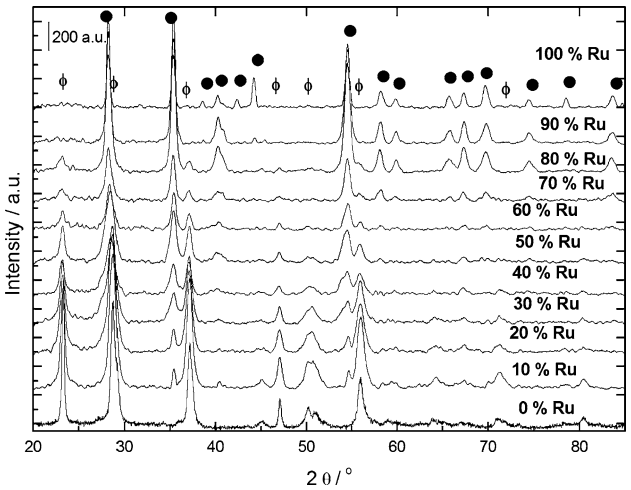

Fig. 1 XRD pattern obtained from RuO_2/Ta_2O_5 powders as a function of Ru loading. (ϕ) Ta_2O_5 (orthorhombic) [JCPDS—25-0922] and (●) RuO_2 (rutile) [JCPDS—40-1290]. Conditions: 700 °C for 5 h under air

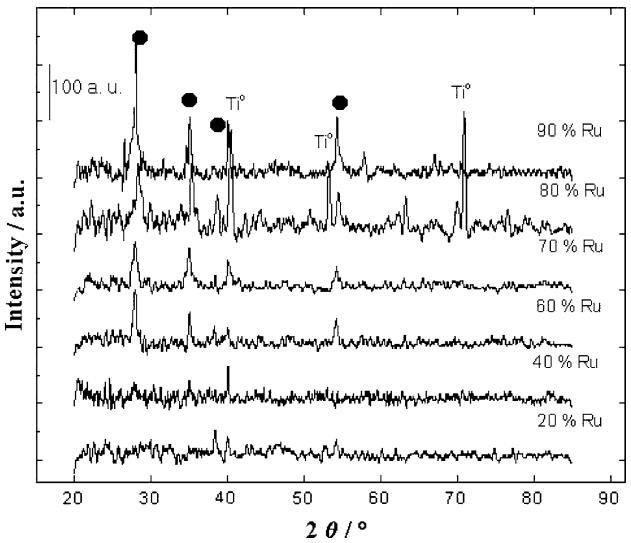

Fig. 2 XRD pattern obtained from thin films of RuO_2/Ta_2O_5 on a Ti substrate as a function of Ru loading. (●) RuO_2 (rutile) [JCPDS—40-1290] and Ti (metallic) [JCPDS—01-1197]. Conditions: 450 °C for 1 h under 5 dm^3 min^{-1} O_2-flux

to observe diffraction peaks for any of the oxides present in the thin film. This suggests the formation of an amorphous phase. This result is expected based on thermogravimetric data showing that the tantalum oxide formation occurs at temperatures higher than 450 °C [27] and complete Ta_2O_5 crystallization occurs at temperatures around 700 °C [3, 27]. A similar result was observed for RuO_2–Ta_2O_5 films prepared by SD [4].

Ru-rich films (Ru ≥ 50 at.%) show the main characteristic reflection peaks of RuO_2 as observed in Fig. 1 for powder samples; once again Ta_2O_5 reflections could not be observed. These results show that at the temperature used

for the thin films preparation the coatings obtained were a mixture of crystalline RuO_2 and amorphous Ta_2O_5 phases.

The unit cell parameters for the crystalline phases present in the Ru–Ta powders and thin films are presented in Table 1. The values for the RuO_2 phase are illustrated in Fig. 3. It can be seen that for Ru-rich samples (≥50 at.%) in powder form the values for crystal parameter, *a*, are in agreement with the literature [24, 25]. On the other hand, higher dispersion is observed for Ta-rich compositions (Ru ≤ 40 at.%). This result suggests a better interaction between the RuO_2 and Ta_2O_5 phases in these compositions. For the *c* parameter, a shift from the literature values is observed [24]. Similar behavior has been seen with other oxides, which is believed to be related to the non-equilibrium state obtained by the preparation method [25]. For thin films, the *c*-values are close to literature values [24] and the highest discrepancy was observed for 50 at.% Ru loading, as noted previously [4]. The difference in the unit cell parameters observed for the powder sample and the thin film sample is most likely due to an interaction between the oxide coating and the metallic substrate in the thin film sample and partial crystallization of the oxides caused by lower firing temperatures (thin film).

The unit cell parameters obtained for RuO_2–Ta_2O_5 are observed to change with the preparation methodology. The values shown here for the DPP-route presented an increase in the phase disordered structure (solid solution) compared with the former RuO_2–Ta_2O_5 oxide prepared using the SD-method [4]. The two preparation methods also result in different crystallographic parameters from the pure oxide. This is good evidence that the DPP method promotes better interaction in the RuO_2–Ta_2O_5 oxide mixture.

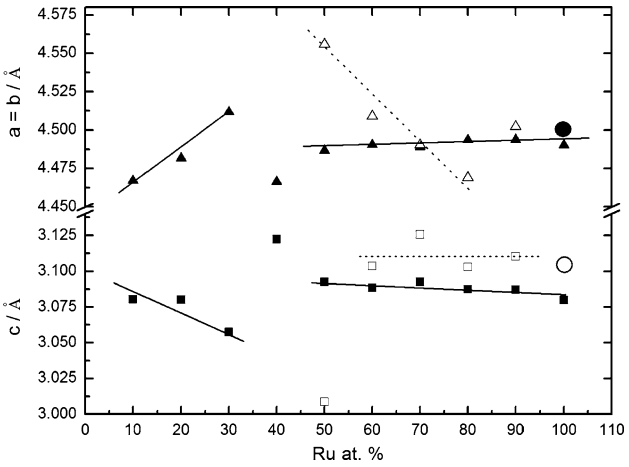

Fig. 3 Unit cell parameters as a function of Ru loading for: (close symbols) powder and (open symbols) thin film samples. (▲ and △) a = b and (■ and □) c parameters (● and ◯) Ref. [24]

Independent of reflection planes, the powder samples containing between 30 and 50 at.% Ru exhibit average crystallite sizes of 5.6–8.4 nm which is smaller than the other compositions investigated. For thin films, the smallest *D*-values, ranging from 7.4 to 11.2 nm, were obtained with 70–80 at.% Ru loading. The thin film values are of the same order of magnitude as those obtained by SD [4]. This behavior suggests that the crystallite size for Ru-rich

Table 1 Unit cell parameters for RuO_2–Ta_2O_5 solid solution and saturated solid solution as a function Ru loading

Sample	Ru at.%	*a* = *b* (Å)		*a* (Å)	*c* (Å)			*b* (Å)
		RuO_2 saturated	Solid solution	Ta_2O_5 saturated	RuO_2 saturated	Solid solution	Ta_2O_5 saturated	Ta_2O_5 saturated
Ref. 24	100		4.499			3.107		
Powder	100		4.490			3.079		
	90		4.494			3.087		
	80	4.494		5.892	3.088		3.866	40.472
	70	4.489		6.192	3.093		3.869	39.777
	60	4.490		6.013	3.089		3.863	40.667
	50	4.487		6.277	3.093		3.857	40.039
	40	4.466		6.247	3.123		3.858	39.956
	30	4.512		6.221	3.058		3.853	40.062
	20	4.482		6.227	3.080		3.853	40.088
	10	4.467		5.993	3.080		3.860	40.032
	0		6.141			3.883		40.031
Ref. 24	0		6.198			3.888		40.290
Thin film	90		4.502			3.115		
	80	4.469			3.103			
	70	4.490			3.126			
	60	4.501			3.104			
	50	4.556			3.009			

samples is independent of the preparation method. Comparing the reflection planes of Ta_2O_5, it was observed that, with the exception of the 001 plane, *D*-values increase as a function of Ru content. These results suggest that the Ru atom promotes larger Ta_2O_5 crystallites. Ta appeared to have no effect on RuO_2 structure or crystallite size.

3.2 XPS analysis

The XPS spectra recorded for Ti/RuO_2, Ti/Ta_2O_5 and Ti/RuO_2–TaO_5 (Ru:Ta = 30:70 and 80:20) electrodes are shown in Fig. 4. All major features of Ru, Ta and O are visible. The spectra indicate that the surfaces are clean and free from pronounced amounts of contaminants except carbon. Ti was also detected in one specific case: Ti/Ta_2O_5.

Figure 5 shows the core level peaks for the Ru 3d (A), Ta 4f (B) and O 1s (C) regions. The most prominent feature of the Ru $3d_{5/2}$ core level peak is located at 280.3–280.8 eV and is assigned to Ru(IV) (Fig. 5a). The position of the corresponding Ru $3d_{3/2}$ core level peak is at 284.0–284.3 eV (the precise determination of the Ru doublet parameters has been obtained by fitting of simulated curves—see Fig. 6). The core level peaks and separation between these peaks (~4.0 eV) agrees well with reported values [28–31]. Ru-rich samples (Fig. 6b) also show the Ru 3d core level peak located at 282.5 eV assigned to Ru(VI) [29]. Moreover, no shift in the peak positions (e.g. binding energy, BE) of the main Ru $3d_{5/2}$ core level peaks is observed as Ta was added to the thin film. This reveals that the introduction of Ta into the coating does not lead to significant changes in the binding of Ru. The O/Ru ratio for the sample Ti/RuO_2 is close to 3.2, larger than the value of 2.0 expected from stoichiometry of the compound.

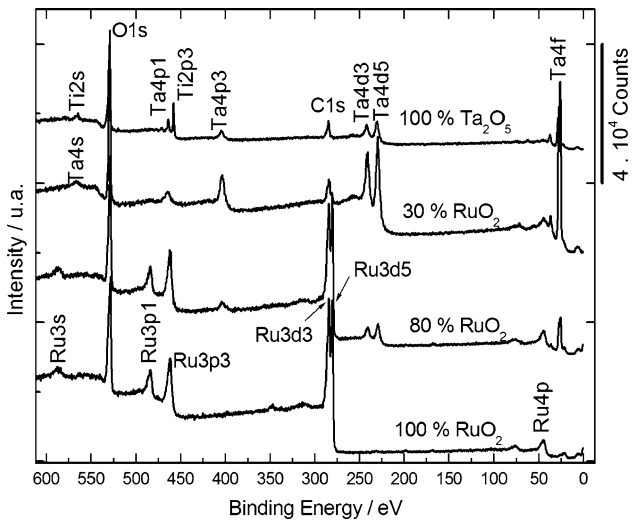

Fig. 4 General XPS spectrum recorded for different electrode compositions

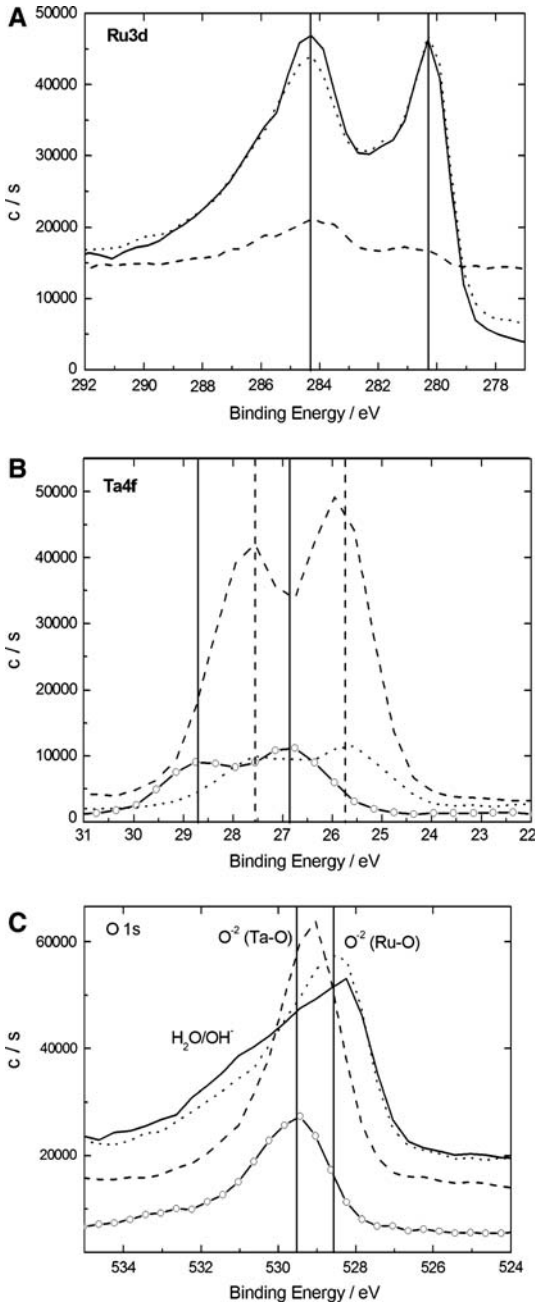

Fig. 5 Core level peaks from different electrode compositions. (Solid line) Ti/RuO_2; (-o-) Ti/Ta_2O_5; (dash line) Ti/RuO_2–Ta_2O_5 (Ru:Ta = 30:70) and (dot line) Ti/RuO_2–Ta_2O_5 (Ru:Ta = 80:20). Ru 3d (**a**), Ta4f (**b**) and O 1s (**c**) regions

The Ta $4f_{7/2}$ core level peak for Ti/Ta_2O_5 is positioned at a binding energy of 26.9 eV which is the typical Ta chemical state in Ta_2O_5 as shown in Fig. 5b [32, 33]. The most interesting characteristic of this spectrum is that there is almost no interference in the shape of the Ta $4f_{7/2}$ core level peaks with the Ti-base. In fact, no shift in the peak position (BE) of the main Ta $4f_{7/2}$ peak is observed. The O/Ta ratio is close to 4.4, larger than the value of 2.5 expected from stoichiometry of the compound. This behavior can be

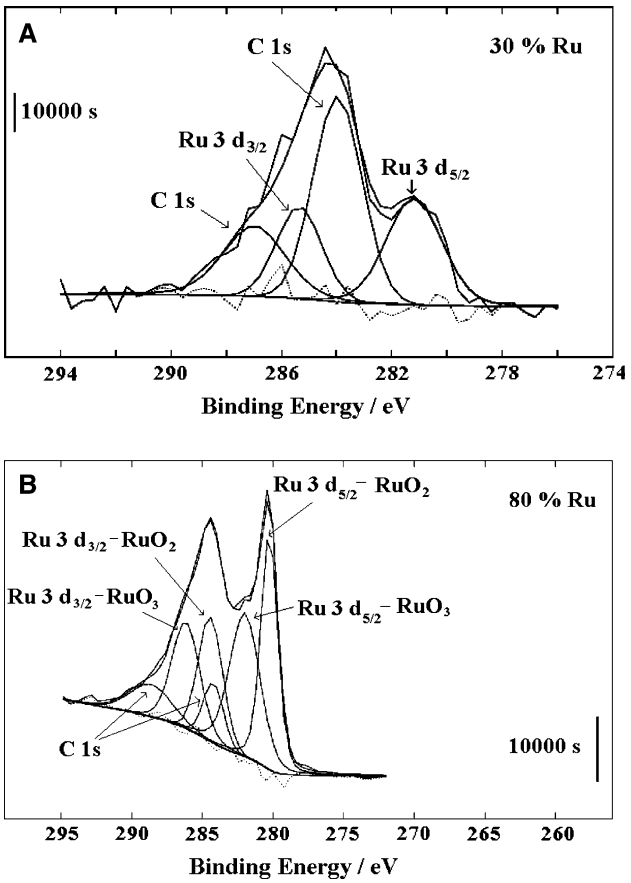

Fig. 6 Ru 3d core level peak from Ti/RuO_2–Ta_2O_5 system. (**a**) Ru:Ta = 30:70 at.% and (**b**) Ru:Ta = 80:20 at.%

explained by presence of TiO_x in the coating, which can lead to an increase of the O concentration.

Unlike the prior observations regarding the Ru 3d peaks, the introduction of Ru to the coating did result in a shift in the Ta $4f_{7/2}$ peak position. The Ta $4f_{7/2}$ peak shifted to lower binding energies (e.g. 25.6–26.0 eV), indicating that the presence of the Ru affects the Ta chemical state. The Ta 4d doublet peaks also show a shift toward lower binding energies ($\sim$1.2 eV shift on both peaks) with the introduction of Ru to the thin films. This is indicative of the existence of electronic effects, suggesting that there is an electron charge transfer from Ru to Ta. Both of these are in agreement with XRD-results that show *D*-values increasing as a function of Ru percentage.

The O 1s core level peak is most probably formed by three binding energies associated with Ru–O at 528.6 eV, Ta–O at 529.5 eV and oxygen in OH^- ions and/or absorbed water at 531.5 eV [29–32] as shown in Fig. 5c. No change in O 1s binding was observed as a function of thin film composition.

The C 1s core level peak at 283.9 eV was observed for all samples; this peak is located in the vicinity of the Ru $3d_{5/2}$ peak. The large broad peak seen in the region between 283 and 288 eV most probably originates from various carbon-based function groupings [30, 31]. It is believed that the surface carbon is most likely from handling contamination and not residual carbon from the DPP-procedure.

3.3 SEM and EDS analysis of the RuO_2–Ta_2O_5 electrodes

Figure 7 shows representative SEM images of freshly prepared Ti/RuO_2–Ta_2O_5 electrodes. Films of RuO_2–Ta_2O_5 binary composition presented a rough mud-cracked morphology (2–5 μm) [34–36]. Pure oxides (7A and 7D) are fairly compact and smooth.

In order to investigate the internal structure of the electrodes, samples were sputtered with ionized argon with a Zalar rotation of 1 rpm to remove $\sim$50 Å from the surface of the coating. The sputter rate is calibrated to Ta_2O_5 material, and may be different for the oxides examined. The sputtered area is $\sim 2 \times 2$ mm, but with the rotation, a circular spot is created. Pure oxides exhibit nanoporous characteristics, which would be expected as previous work on these types of films has indicated. The binary oxides do not exhibit nanoporosity (even at 50,000×), the only visible defects being mud-cracks created during the drying and firing of the sample. The lack of nanoporosity maybe due to the formation of an amorphous phase (Ta_2O_5) surrounding crystallites of RuO_2. However, this is only conjecture and more work is needed to confirm this hypothesis.

After accelerated life tests (ALT), SEM micrographs of Ta-rich thin films indicate no change in morphology, suggesting that there was no significant loss of material by erosion/corrosion during ALT. However, for Ru-rich thin films (Ru $\geq$ 50 at.%) a slight erosion/corrosion process was observed. The dissolution of Ru during ALT was confirmed by a color change in the electrolyte solution during ALT. The solution changed from colorless to gray indicating that the film was partially dissolved during long-term operation at high current densities. A similar result was observed for electrodes prepared by SD [4, 37].

Table 2 gives the results obtained by EDS for thin films investigated in this work before and after ALT. The experimental data shows excellent agreement with nominal compositions before ALT. After ALT, Ta-rich thin films ($\geq$80 at.%) did not show a preferential loss of Ru to Ta and may indicate minimal coating loss. However, thin films containing higher amounts of Ru ($\geq$30 at.%) show a loss of Ru preferentially to Ta. These results confirm the erosion/corrosion observed in SEM images for these compositions. Moreover, we can infer that Ru might be transferred to the solution phase due to a corrosion process (electrochemical oxidation to soluble RuO_4^{2-}) as visually indicated by a change in ALT solution color [38].

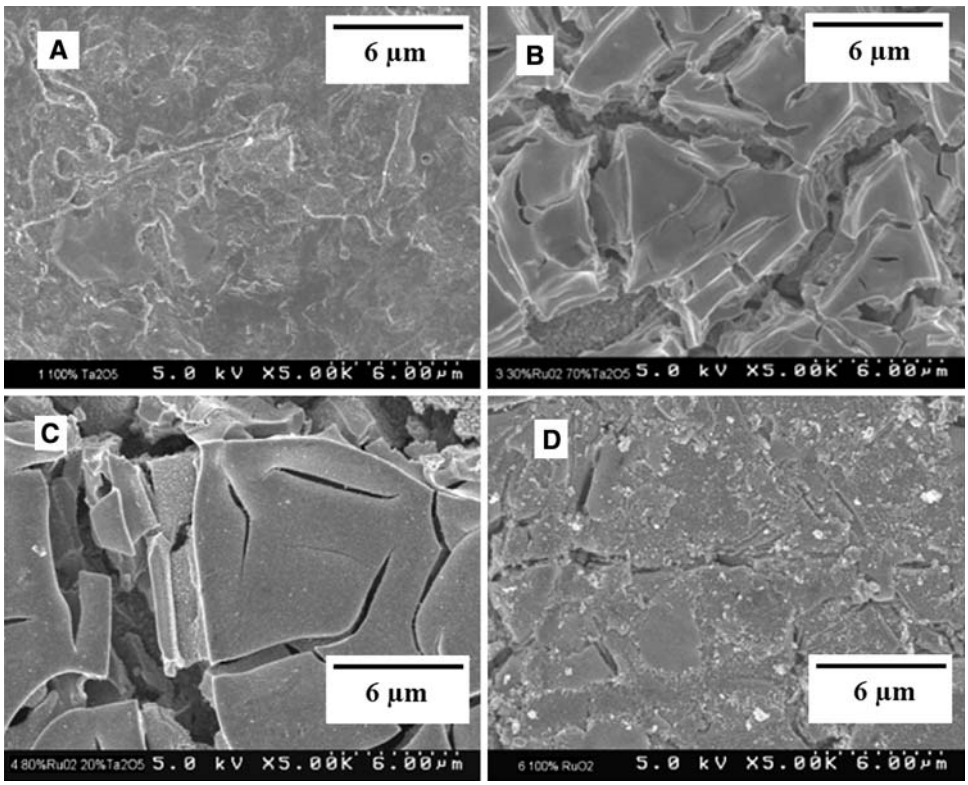

Fig. 7 Representative SEM images (5,000×) for electrodes of nominal compositions: (**a**) Ti/RuO_2–Ta_2O_5—Ru:Ta = 100:0 at.%; (**b**) Ti/RuO_2–Ta_2O_5—Ru:Ta = 30:70 at.%; (**c**) Ti/RuO_2–Ta_2O_5—Ru:Ta = 80:20 at.% and (**d**) Ti/RuO_2–Ta_2O_5—Ru:Ta = 0:100 at.%

Table 2 Nominal and experimental compositions of the Ru/Ta coatings prepared by DPP before and after accelerated life tests

Atomic percentage nominal and experimental[a]				Lifetime (h)	
Before ALT		After ALT		DPP	SD[b]
Ru	Ta	Ru	Ta		
(10) 10.8	(90) 89.2	9.9	90.1	0.04	0.07
(20) 19.5	(80) 80.5	22.1	77.9	0.08	
(30) 34.2	(70) 65.3	19.6	80.4	1.2	0.3
(40) 28.0	(60) 72.0	19.7	80.3	2.9	
(50) 49.9	(50) 50.1	29.1	70.9	4.0	4.0
(60) 58.4	(40) 41.6	30.4	69.6	6.3	
(70) 71.4	(30) 28.6	42.0	58.0	11.9	
(80) 76.6	(20) 23.4	56.0	44.0	16.0	8.5
(90) 90.2	(10) 9.8	66.7	33.3	18.5	

( ) Atomic percentage nominal

[a] Data obtained by EDS overall analyses (100×)

[b] Data obtained from Ref. [4]

3.4 Cyclic voltammetry (CV)

Figure 8a shows the voltammetric curves obtained for freshly prepared electrodes. The voltammetric curves are characterized by the presence of the Ru(III)/Ru(IV) [4, 9–14, 19, 25, 34, 37, 38] solid state surface redox peaks, which lie between +0.5 and +1.0 V vs. RHE. The CV plots are in close agreement with those previously reported for other Ru-valve metal systems [4, 9–14, 19, 25, 34, 37, 38]. Comparing Fig. 8a with the previous results for Ti/RuO_2–Ta_2O_5 prepared by standard methods [4], one observes that there is not much difference concerning the position of the redox peaks. However, when one compares the voltammetric charge, q, for the same electrode composition obtained as a function of the preparation method it is found that the electrodes prepared by DPP have charge values at least two times higher than those prepared by SD [4].

The voltammetric charge, q_a*, measured between 0.2 and 1.1 V vs. RHE, increases slowly up to 60 at.% Ru and shows a steep increase for Ru-rich films (Fig. 8b). Thin films containing 80 at.% Ru exhibit the greatest active electrochemical area. As expected, the greatest active surface area occurs at the composition that produced the smallest crystallite size as measured by XRD.

3.5 Accelerated life test (ALT)

Figure 9 shows a representative E–t curve for ALT of the Ti/RuO_2–Ta_2O_5 system prepared through DPP. Independent of the electrode investigated, all curves display a slow increase in potential during the first part of the ALT (~85% of the total life), followed by an abrupt increase in potential at the end of the experiment (~last 15% of ALT). This behavior indicates a rise in resistance in the electrode structure. The resistance increase could result from the loss

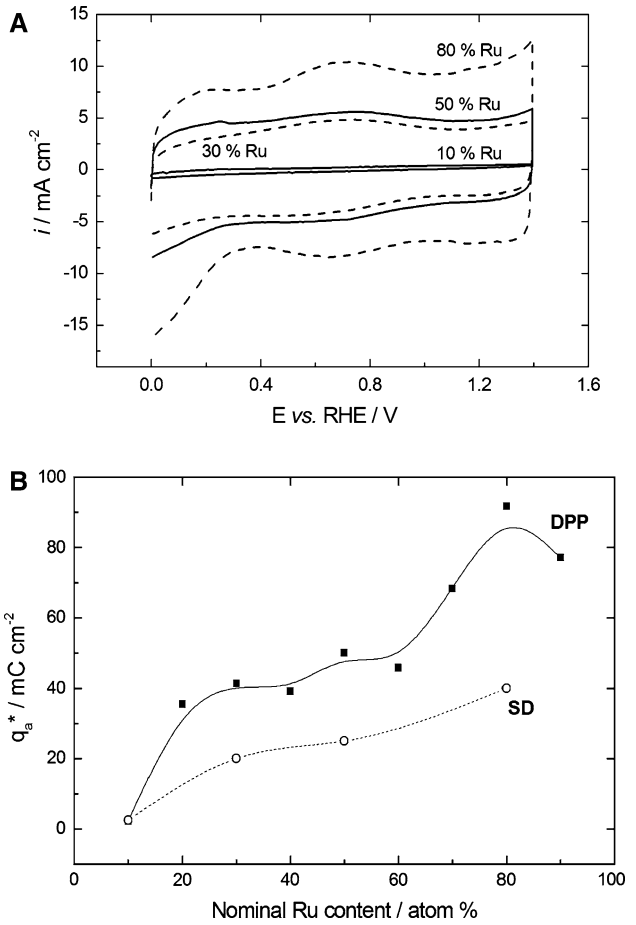

Fig. 8 (**a**) Voltammetric curves at 100 mV s^{-1} in 0.5 mol dm^{-3} H_2SO_4 of the Ti/RuO_2–Ta_2O_5 system. (**b**) Voltammetric charge as a function of Ru loading and electrode preparation methodology

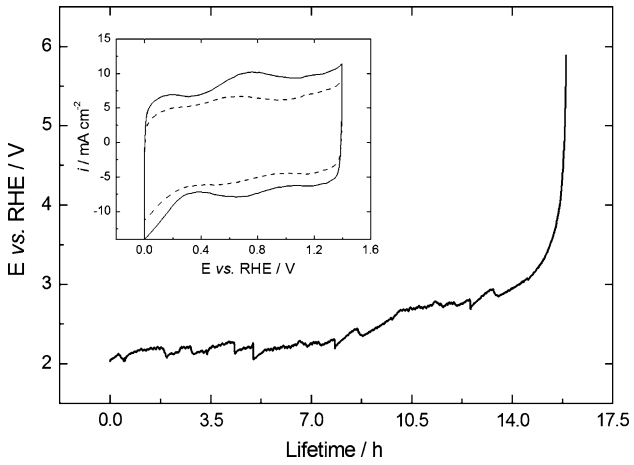

Fig. 9 Representative potential-time curves of the Ti/RuO_2–Ta_2O_5 (Ru:Ta = 80:20 at.%) electrode. Galvanostatic conditions 750 mA cm^{-2}; 0.5 mol dm^{-3} at T = 80 °C. Inset: Voltammetric curves of Ti/RuO_2–Ta_2O_5 (Ru:Ta = 80:20 at.%) composition (solid line) before and (dash line) after ALT test

of Ru in the top layers of the electrode and/or by the formation and growth of a non-conductive oxide film between the titanium substrate and electrocatalytic coatings. While it is known by EDS and the changing color of the testing solution that Ru was lost from the coating, the location of Ru loss was not determined.

The voltammetric charge at the end of the ALT test for all electrode compositions decreased by 30–50% as compared to a fresh electrode (see inset in Fig. 9). The presence of the Ru(III)/Ru(IV) peak along with the EDS data indicates that a portion of the deposited oxide layer is still present after the ALT. Therefore, it can be concluded that the main reason for deactivation is the progressive growth of an insulating TiO_x layer. A similar conclusion was obtained for the same electrodes prepared by SD, which were investigated by electrochemical impedance spectroscopy (EIS) [37].

Table 2 shows the average ALT values for the RuO_2–Ta_2O_5 system as a function of the amount of Ru in the film for both the DPP and SD methods [4]. Comparing the methods, electrode service life was improved for 30 and 80 at.% Ru compositions by changing the preparation methodology (DPP instead SD). Interestingly, 50 at.% Ru did not show a difference in lifetime based on preparation method. As shown before by us [4], the RuO_2–Ta_2O_5 system is much more stable than RuO_2–TiO_2 under galvanostatic conditions [7, 8] and its use as an anode should be more widespread.

Figure 10 shows the variation in the amount of Ru in mg cm^{-2}, obtained by EDS, before and after ALT for the Ti/RuO_2–Ta_2O_5 electrodes prepared by DPP and SD. Taking into account equimolar compositions, it is observable that Ta-rich thin films show similar loss of Ru for both preparation methods. On the other hand, Ru-rich films exhibit a higher loss of Ru from the active layer for electrodes prepared by DPP than SD. This most likely resulted from DPP electrodes operating for longer times before the onset of passivation.

4 Conclusions

This work has demonstrated that the DPP preparation route can promote a significant increase in the lifetime for RuO_2–Ta_2O_5 coated titanium anodes. In spite of Ru loss after ALT (5–60%), a considerable amount of Ru is observed after exhaustive electrolysis (12–60 at.% Ru). Thus, the deactivation mechanism for this system is mainly controlled by passivation due to the formation of an insulating TiO_x interlayer.

XRD results indicate solid solution formation in a small range of RuO_2–Ta_2O_5 composition (0–10 at.% Ru and 80–100 at.% Ru). Changes in the preparation method promote changes in the unit cell volume of the crystallites. The DPP

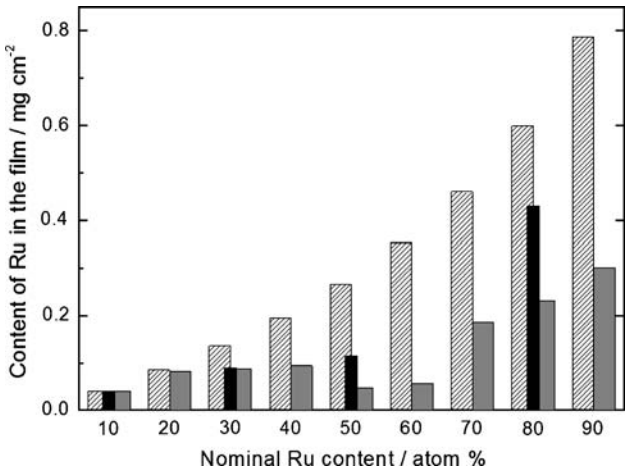

Fig. 10 Content of Ru in the film as a function of the nominal composition of electrodes before (striped) and after ALT (gray) DPP, (black) SD from [4]. Galvanostatic conditions 750 mA cm^{-2}; 0.5 mol dm^{-3} at $T = 80$ °C

method leads to smaller volumes when compared with SD. XPS data revealed that the introduction of Ta in the coating does not lead to significant change in the Ru chemical state (Ru $3d_{5/2,}$ but that introduction of Ru does change the Ta chemical state.

Acknowledgements Financial support from FAPESP, CNPq and the Center of Advanced Separation Technologies is gratefully acknowledged. J. Ribeiro also acknowledges a PhD fellowship (FAPESP -# 02/06465-0).

References

1. Vercesi GP, Rolewicz J, Comninellis C, Hinden J (1991) Thermochim Acta 176:31
2. McKinley KA, Sandler NP (1996) Thin Solid Films 291:440
3. Ushikubo T (2000) Catal Today 57:331
4. Ribeiro J, De Andrade AR (2004) J Electrochem Soc 151:D106
5. Chang TY, Wang X, Evans DA et al (2002) J Power Sources 110:138
6. Newalkar BL, Komarneni S, Katsuki H (2002) Mater Lett 57:444
7. Lin SM, Wen TC (1993) J Appl Electrochem 23:487
8. Pelegrino RRL, Vicentin LC, De Andrade AR et al (2002) Electrochem Commun 4:139
9. Ardizzone S, Carugati A, Trasatti S (1981) J Electroanal Chem 126:287
10. DeBattisti A, Lodi G, Nanni L et al (1997) Can J Chem 75:1759
11. Trasatti S, Buzzanca G (1971) J Electroanal Chem 29:1
12. Coteiro RD, Teruel FS, Ribeiro J et al (2006) J Braz Chem Soc 17:771
13. Tilak BV, Birss VI, Wang J et al (2001) J Electrochem Soc 148:D112
14. Trasatti S (1991) Electrochim Acta 36:225
15. Terezo AJ, Pereira EC (2002) Mater Lett 53:339
16. Pechini MP, Adams N (1967) US Patent 3, 330, 697:1
17. Santos MC, Terezo AJ, Fernandes VC et al (2005) J Solid State Electrochem 9:91
18. Ronconi CM, Pereira EC (2001) J Appl Electrochem 31:319
19. Forti JC, Olivi P, De Andrade AR (2001) Electrochim Acta 47:913
20. Profeti D, Lassali TAF, Olivi P (2006) J Appl Electrochem 36:883
21. Ribeiro J, Alves PDP, De Andrade AR (2007) J Mater Sci 42:9293
22. Garavaglia R, Mari CM, Trasatti S (1984) Surf Technol 23:41
23. Cullity BD (1978) Elements of X-ray diffraction. Addison-Wesley, San Francisco
24. Powder Diffraction File: 40-1290; 25-0922; 01-1197 (1996) Joint Committee on Powder Diffraction Standards, International Center for Diffraction Data, Vol. PDF2-46, Pennsylvania, USA
25. Nanni L, Polizzi S, Benedetti A et al (1999) J Electrochem Soc 146:220
26. Hume-Rothery W, Smallman RE, Hayworth CW (1969) The structure of metals and alloy. London
27. Kristof J, Szilagyi T, Horvath E et al (2005) Thin Solid Films 485:90
28. Kotz R, Stucki S (1986) Electrochim Acta 31:1311
29. Shen JY, Adnot A, Kaliaguine S (1991) Appl Surf Sci 51:47
30. Rochefort D, Dabo P, Guay D et al (2003) Electrochim Acta 48:4245
31. Wang CC, Hu CC (2005) Carbon 43:1926
32. Atanassova E, Dimitrova T, Koprinarova J (1995) Appl Surf Sci 84:193
33. Kuo Y (1992) J Electrochem Soc 139:579
34. Trasatti S, Lodi G (1981) Properties of conductive metal oxides with rutile type structure. Elsevier, Amsterdam
35. Da Silva LA, Alves VA, Da Silva MAP et al (1997) Electrochim Acta 42:271
36. Ribeiro J, De Andrade AR, Bento CAS et al (2003) Acta Microsc 12:115
37. Ribeiro J, De Andrade AR (2006) J Electroanal Chem 592:153
38. Kotz R, Stucki S, Scherson D et al (1984) J Electroanal Chem 172:211